

# We are IntechOpen, the world's leading publisher of Open Access books Built by scientists, for scientists

6,900

Open access books available

186,000

International authors and editors

200M

Downloads

Our authors are among the

154

Countries delivered to

TOP 1%

most cited scientists

12.2%

Contributors from top 500 universities



WEB OF SCIENCE™

Selection of our books indexed in the Book Citation Index  
in Web of Science™ Core Collection (BKCI)

Interested in publishing with us?  
Contact [book.department@intechopen.com](mailto:book.department@intechopen.com)

Numbers displayed above are based on latest data collected.  
For more information visit [www.intechopen.com](http://www.intechopen.com)



# Experimental Studies on Doped and Co-Doped ZnO Thin Films Prepared by RF Diode Sputtering

Krasimira Shtereva<sup>1,2</sup>, Vladimir Tvarozek<sup>2</sup>, Pavel Sutta<sup>3</sup>,  
Jaroslav Kovac<sup>2</sup> and Ivan Novotny<sup>2</sup>

<sup>1</sup>University of Rousse

<sup>2</sup>Slovak University of Technology in Bratislava

<sup>3</sup>New Technologies Research Center, West Bohemian University

<sup>1</sup>Bulgaria

<sup>2</sup>Slovakia

<sup>3</sup>Czech Republic

## 1. Introduction

For decades zinc oxide (ZnO) has been in the spotlight due to its unique combination of semiconductor, piezoelectric, optical, and magnetic properties, which open perspectives for wide range of applications from optoelectronic and transparent electronic devices (Ohta & Hosono, 2004), surface and bulk acoustic wave devices and piezoelectric transducers (Wang et al., 2008), spintronics (Ji et al., 2008), to chemical and gas sensors (Carotta et al., 2009), and solar cells (Ganguly et al., 2004). Great industrial advantages of ZnO are its eco-friendly nature, wide abundant sources and low costs of metal Zn.

ZnO is a group II-VI semiconductor with a direct band gap of 3.37 eV at room temperature, which can be modified (~3 eV– 4 eV) via extrinsic doping with either cadmium (Cd) or magnesium (Mg). By its semiconductor properties ZnO is similar to gallium nitride (GaN) (Table 1).

Wide band gap semiconductor	ZnO	GaN	ZnSe
Crystal structure	wurtzite	wurtzite	zinc-blende
Energy gap at RT, ( $E_g$ ), (eV)	3.37	3.4	2.7
Exciton binding energy (meV)	60	21	20
Dielectric constant	8.75	9.5	7.1
Melting point (°C)	1975	1700	1100
Lattice constant (Å)			
a-axis (Å)	3.25	3.19	5.67
c-axis (Å)	5.21	5.19	-

Table 1. Comparison of some basic properties of ZnO, GaN and ZnSe (Tüzemen & Gür, 2007)

Both materials have wurtzite crystal structure and very closed values of energy gap, lattice constants and thermal expansion coefficients. Therefore, ZnO can provide a high quality substrate for GaN.

Remarkable optical qualities (the width of band gap and large exciton binding energy of 60 meV), enable application for light emitting diodes (LEDs) and UV semiconductor lasers, which are devices with great commercial potential.

Besides, ZnO exhibits impressive stability of its properties when exposed to temperatures up to 700 K and radiation and hence, ZnO devices are suitable for space applications.

Resistance dependence on temperature, pressure and illumination can be utilized in temperature and pressure sensors and fire alarm.

Undisputable advantage of ZnO over GaN and ZnSe is the lowest price of single crystal wafers ZnO (1 side polish, 10x10 mm), fabricate from Wafer World Inc. (Fig. 1).

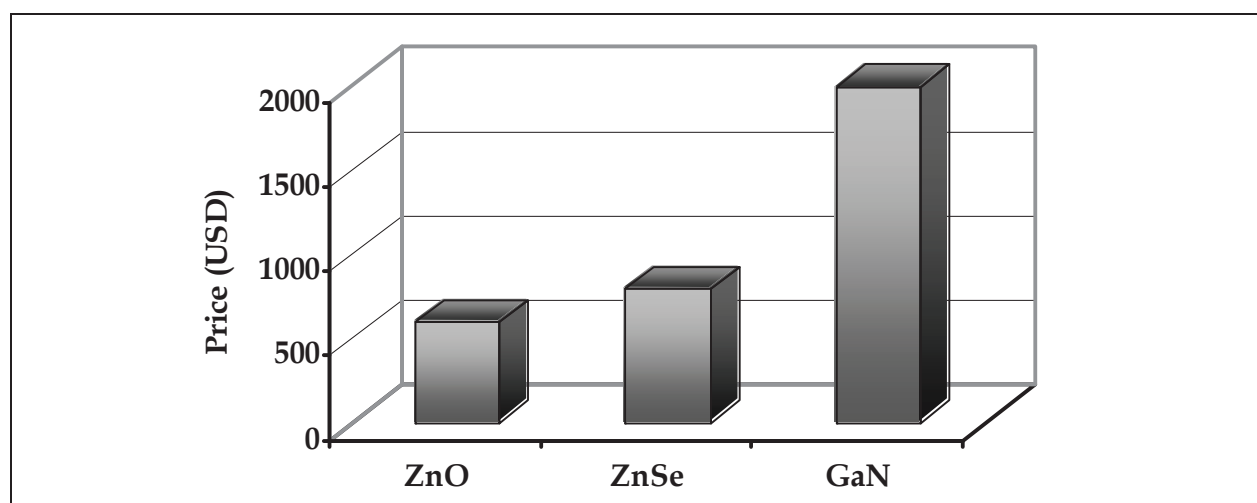


Fig. 1. Comparison between the price of ZnO, GaN and ZnSe wafers (<http://www.waferworld.com/>)

Zinc oxide can provide an alternative to other transparent conductive oxides (TCOs), (tin-doped indium oxide ( $\text{In}_2\text{O}_3:\text{Sn}$ ) (ITO) and antimony-doped tin oxide ( $\text{SnO}_2:\text{Sb}$ )), which are widely used as transparent electrodes for liquid crystal displays (LCDs), organic light-emitting diodes (OLEDs), and in photovoltaic solar cells. ZnO has higher conductivity than tin oxide and is readily etchable than ITO. Furthermore, zinc is an inexpensive and abundant metal, whereas indium is a rare metal, and parallel to the growing market for flat panel displays grow worries over its depletion and stable supplies.

The remarkable properties of zinc oxide along with: (i) presence of high quality single crystals; (ii) ability to grow ZnO thin films; (iii) ability to dope ZnO and this way to modify its physical properties; (iv) ability to metalize for ohmic contacts and interconnections, make ZnO one of the most promising semiconductor materials of the new millennium.

Our work has been motivated by the optoelectronic applications of ZnO and the need of both, high quality *p*-type and *n*-type materials to realize active devices. In this chapter we will present our research on the growing and characterizing of *p*-type ZnO thin films, prepared by radio frequency (RF) diode sputtering, mono-doped with nitrogen (ZnO:N), and co-doped with aluminium and nitrogen (ZnO:Al:N). Important parameters such as crystallite size ( $D$ ), strain ( $\epsilon$ ), texture orientation, type and carrier concentration ( $n/p$ ), carrier mobility ( $\mu$ ) and resistivity ( $\rho$ ), have to be determined when assessing ZnO quality. In the

following sections the reader will find experimental results and analysis of these micro structural and electrical parameters, and a discussion over their interconnection. We do believe that this research contributes to the better understanding of doping behavior and *p*-type conductivity in ZnO.

## 2. Doping ZnO

Doping is fundamental to controlling the properties of the semiconductors and to obtaining of new multifunctional materials. There is a wide variety of well developed doping methods, including diffusion, ion implantation, and in situ doping with epitaxial growth. The pure elemental semiconductors, such as silicon (Si) or germanium (Ge), tend to be electrically intrinsic. They can be readily *n*- or *p*-type doped using extrinsic dopants, such as boron (B) or phosphorous (P), therefore, they are denoted symmetrically doped. The doping and re-doping of the same silicon crystal from *n*- to *p*-type and back again is very common during the device fabrication. On the contrary, the wide band gap semiconductors, including ZnO, are denoted asymmetrically doped, i.e., they can be doped easily either *n*-type or *p*-type but not both. This asymmetry has been explained with (i) the low or limited solubility of the desirable dopants; (ii) the high activation energies of these dopants, (iii) the tendency to form spontaneously compensating defects, and (iv) hydrogen acting as an unintentional extrinsic donor.

Zinc oxide exhibits asymmetry in doping and *n*-type conducting ZnO can be readily obtained via either native or extrinsic donor defects whereas *p*-type doping turned out to be more difficult. Density functional theory identifies as donors two native point defects in ZnO structure, the oxygen vacancy ( $V_O$ ) and the zinc interstitial ( $Zn_i$ ) (Look et al., 2003). One of them, Zn interstitial, is a shallow donor, whereas O vacancy is a deep donor. The cation vacancies are expected to create acceptor levels in most of group II-VI semiconductors and hence Zn vacancy ( $V_{Zn}$ ), a part of  $Zn_i$ -  $V_{Zn}$  Frenkel pair, is an important acceptor in ZnO. Since  $Zn_i$  is expected to have high formation energy it puts the question whether (only) this defect is responsible for the donors' concentration in un-doped *n*-type material. Theoretical studies of Van de Walle found hydrogen is a shallow donor in ZnO (Van de Walle, 2000).

### 2.1 ZnO *n*-type doping

Conductive ( $\rho \sim 10^{-4} \Omega\text{cm}$ ) and transparent ( $T > 80\%$ ) *n*-type ZnO thin films have significant commercial impact due to their use as transparent electrodes for flat panel displays, organic light emitting devices and in solar cells. They can be obtained via doping of ZnO with either group III elements, aluminum (Al), gallium (Ga) or indium (In), as a substitution for Zn, or group VII elements, chlorine (Cl) and iodine (I) as a substitution for O, in the crystal lattice. Almost metal conductivity ( $\rho = 4.6 \times 10^{-4} \Omega\text{cm}$ , sheet resistance  $R_s = 32 \Omega/\square$ ) was reported for aluminum - doped ZnO films (ZnO:Al), deposited by middle-frequency (MF) alternative magnetron sputtering (Fu et al., 2004), and DC magnetron sputtering ( $\rho = 9 \times 10^{-4} \Omega\text{cm}$ ) (Guillén & Herrero, 2006). Their low resistivity was combined with high visible transparency (85 - 90 %). By changing the sputter pressure and the film thickness were modified physical properties and obtained Ga-doped films (ZnO:Ga) with resistivity of  $2.6 \times 10^{-4} \Omega\text{cm}$ , Hall mobility of  $18 \text{ cm}^2/\text{Vs}$  and the carriers concentration of  $1.3 \times 10^{21} \text{ cm}^{-3}$  (Assunção et al., 2003, Fortunato et al., 2004). It was found that mobility and grain size were linearly dependent, which resulted in high mobility in films with larger crystalline grain size. Optical transmittance (80 - 90 %) depends on both, thickness and sputtering pressure

and its changes are consistent with the changes of the electrical parameters. Other deposition parameter with major influence on the film's properties is the substrate temperature ( $T_s$ ). Textured ZnO:Ga films with a strong preferential orientation can be deposited only at optimum temperature (Song et al., 2002). ZnO thin films doped with In, Ga and Al were utilized in amorphous silicon solar cells (Nunes et al., 2002). The best parameters showed the cells with ZnO:In films.

Rare-earth elements yttrium (Y) and scandium (Sc) make efficient donors for producing an *n*-type ZnO material with low resistivity ( $3.1 \times 10^{-4} \Omega\text{cm}$ ) (Minami et al., 2000). Conductivity of ZnO:Sc was higher than that of ZnO:Y and its electrical and optical properties, as well as the thermal stability of resistivity were comparable to those of ZnO:Al.

## 2.2 ZnO p-type doping and co-doping

ZnO can be doped *p*-type intrinsically, through native defects, and extrinsically through impurity doping.

As discussed above, self-compensation by native donor defects and unintentionally introduced impurities (H), prevent the achievement of *p*-type conductivity in un-doped ZnO. Intrinsic *n*-type was changed to moderate *p*-type ZnO ( $\rho = 1250 \Omega\text{cm}$ ,  $\mu = 30 \text{ cm}^2/\text{Vs}$  and  $p = 10^9 \text{ cm}^{-3}$ ), by adjusting the oxygen/argon ratio in the sputtering plasma (Xiong et al., 2002). The authors explained *p*-type conductivity in un-doped ZnO with the increase in the chemical potential of atomic oxygen that lowers the formation energy of the acceptor defects.

On the other hand, the successful extrinsic *p*-type doping is restricted by low solubility and high activation energy of the acceptor dopants in addition to above mentioned compensating species.

Group I elements, such as lithium (Li), as substitution elements for Zn in ZnO crystal lattice, are regarded as suitable acceptors. They create shallow acceptor levels but due to smaller atomic radius than this of the replaced atom, they tend to locate on the interstitial sites and hence, to act as donors. Besides, the larger bond than the Zn-O bond induces the lattice strain that will lower the formation energy of the native donor defect, e.g. O vacancy, which will compensate the dopants (Özgür et al., 2005). Investigations of *p*-type lithium - doped ZnO thin films (ZnO:Li) showed that *p*-type doping by Li is limited from the formation of  $\text{Li}_{\text{Zn}} - \text{Li}_i$  complexes (Zeng et al., 2005). The formation of these complexes can be suppressed by adjusting of the Li content. It was found that low resistivity *p*-type ZnO:Li films ( $\rho = 17 \Omega\text{cm}$ ,  $\mu = 3.47 \text{ cm}^2/\text{Vs}$  and  $p = 1.01 \times 10^{17} \text{ cm}^{-3}$ ), could be obtained at a low Li content and optimum temperature. Resistivity of the films, grown at a high Li content, was high and their absorption edge blue shifted.

Group V dopants, such as nitrogen (N), phosphorus (P) and arsenic (As), which substituting for oxygen in the ZnO crystal lattice, are acceptors as well. Quality *p*-type material was produced by P and As doping, even though their ionic radii are larger than that of O. ZnO *n*-type by arsenic doping (ZnO:As) ( $n \sim 10^{18} \text{ cm}^{-3}$ ), turned to *p*-type ( $p \sim 10^{19} \text{ cm}^{-3}$ ,  $\mu_H = 4.02 \text{ cm}^2/\text{Vs}$ ,  $\rho = 4.4 \times 10^{-2} \Omega\text{cm}$ ) after heat treatment (Ryu et al., 2000, Moon et al., 2005). The phosphorus - doped *p*-type ZnO (ZnO:P) films exhibit a hole concentration of  $5 \times 10^{18} \text{ cm}^{-2}$ , mobility of  $2 \text{ cm}^2/\text{Vs}$  and resistivity of  $2 \Omega\text{cm}$  (Hwang et al., 2005).

### 2.2.1 p-type ZnO by nitrogen-doping

Nitrogen ionic radius is almost the same as that of O and therefore, should match well on the O site. Furthermore, its highest solubility between group V elements and shallower

acceptor levels than phosphorus and arsenic, make nitrogen the preferable candidate for *p*-type doping between group V elements. Promises for successful *p*-type doping are also *p*-type conduction in nitrogen doped ZnSe and high concentration of N<sub>O</sub> acceptor in N-doped ZnO (ZnO:N) thin films grown by plasma-assisted molecular beam epitaxy (P-MBE) (Sun et al., 2006).

Preparation of *p*-type ZnO thin films by nitrogen doping, using different deposition techniques and nitrogen sources, was reported by a number of groups. Electrical parameters of sputtered *p*-type ZnO:N thin films are compared in Table 2.

Reference	Resistivity (Ωcm)	Mobility (cm <sup>2</sup> /Vs)	Concentration (cm <sup>-3</sup> )
(Lu et al., 2003)	4x10 <sup>3</sup>	2.4	4.6x10 <sup>15</sup>
	31	1.3	7.3x10 <sup>17</sup>
	760	1.9	2.4x10 <sup>16</sup>
(Wang et al., 2006)	339	0.08	2.4x10 <sup>17</sup>
	8.34	0.1	7.5x10 <sup>18</sup>
(Yao et al., 2007)	456	0.1	1.2x10 <sup>17</sup>
(Ye et al., 2004)	1200	84.9	6.10 <sup>13</sup>
(Lu et al., 2005)	3.4x10 <sup>4</sup>	8.3	2.18x10 <sup>13</sup>
<b>(Tvarozek et al., 2008)</b>	<b>790</b>	<b>25</b>	<b>3.2x10<sup>14</sup></b>

Table 2. Electrical properties of sputtered *p*-type ZnO:N

Experimental studies suggest a positive role of the acceptor-hydrogen complex (N<sub>O</sub>-H), for suppressing the formation of compensating interstitial defects and for providing *p*-type doping (Lu et al., 2007). Hence, films grown in ammonia (NH<sub>3</sub>) - O<sub>2</sub> ambient were *p*-type with a hole concentration of 7.3x10<sup>17</sup> cm<sup>-3</sup> (Lu et al., 2003). At higher and lower ammonia concentration, the carrier concentration reduces and mobility goes up due to the oxygen deficiency in the growth ambient, which creates large amount of donor defects, such as Zn interstitials and O vacancies. Therefore, it is difficult to obtain carrier concentrations higher than ~ 10<sup>-17</sup> cm<sup>-3</sup> even when the film grows in pure N<sub>2</sub> (Yao et al., 2007). The temperature plays an important role in the activation of the N<sub>O</sub> acceptor and annealing can cause an increase in the hole concentrations (Wang et al., 2006). Indeed, mobility of the annealed samples is higher than of as-deposited ones due to the large grain size and the strong *c*-axis crystalline structure. The XRD patterns of un-doped ZnO thin films show a strong (002) diffraction line, indicating a *c*-axis preferential orientation. Incorporation of nitrogen caused the randomization of the crystallites orientation, which is manifested by appearance of additional lines ((100), (101) and (110)), besides the main (002) line, in the XRD patterns of ZnO:N films (Zhao et al., 2005). The visible transmittance of *p*-type ZnO:N (~ 90 %) is almost the same as for Al-, Ga-, or In-doped ZnO thin films (Lu et al., 2003). The sharp absorption edge appears around 389 nm and shifts towards shorter wavelengths (blue shift) which corresponds to an increase in the carrier concentration.

### 2.2.2 *p*-type ZnO by aluminum-nitrogen co-doping

Theory predicted that co-doping of ZnO simultaneously with acceptors (nitrogen) and donors (Al, Ga or In), enhances incorporation of the N<sub>O</sub> acceptors and supports formation of the shallow N<sub>O</sub> acceptor levels. Hence, co-doping provides better perspectives for obtaining of a *p*-type ZnO material than nitrogen mono-doping.

The electrical parameters of *p*-type N - Al co-doped ZnO thin films are compared in Table 3.

Reference	Resistivity ( $\Omega\text{cm}$ )	Mobility ( $\text{cm}^2/\text{Vs}$ )	Concentration ( $\text{cm}^{-3}$ )
(Ye et al., 2005)	157	0.0711	$5.59 \times 10^{17}$
(Ye et al., 2004)	$1.6 \times 10^2$	0.3	$1.1 \times 10^{17}$
(Yuan et al., 2004)	24.5	0.34	$7.5 \times 10^{17}$
(Lu et al., 2005)	$3.4 \times 10^4$	8.3	$2.18 \times 10^{13}$
(Ge et al., 2004)	78	0.1	$8 \times 10^{17}$
(Zhu et al., 2005)	101	0.05	$1.3 \times 10^{18}$
	160	0.3	$1.1 \times 10^{17}$
<b>(Shtereva et al., 2008)</b>	<b>21</b>	<b>0.4</b>	<b><math>7.8 \times 10^{17}</math></b>

Table 3. Electrical properties of sputtered *p*-type ZnO:N:Al

Indeed, the obtained hole concentration of *p*-type ZnO:N:Al ( $1.1 \times 10^{17} \text{ cm}^{-3}$ ) is more than two orders of magnitude higher than achieved for *p*-type ZnO:N ( $6.7 \times 10^{14} \text{ cm}^{-3}$ ) prepared under the same deposition conditions, which gives an evidence for effectiveness of the co-doping concept (Ye et al., 2004). Estimation of nitrogen incorporation by means of SIMS depth profiles shows the same trend of variation of the N and Al content in the film. Deposition parameters that influence *p*-type doping and the physical properties of ZnO:N:Al are growth ambient and temperature (Lu et al., 2005), and oxygen partial pressure (Ye et al., 2005). In fact, there is optimum temperature or pressure, a kind of temperature/pressure "window" where *p*-type ZnO material can be grown (Yuan et al., 2004). Formation of the compensating donor defects, e.g. nitrogen molecules on the oxygen site,  $(\text{N}_2)_\text{O}$ , can be suppressed by adjustment of the growth temperature. The higher hole concentration of *p*-type ZnO:N:Al films prepared using  $\text{NH}_3$  ( $1.3 \times 10^{18} \text{ cm}^{-3}$ ), compared to this of films doped from  $\text{N}_2\text{O}$  source ( $1.1 \times 10^{17} \text{ cm}^{-3}$ ), is ascribed to hydrogen incorporation into the film together with aluminum and nitrogen that suppresses the formation of the donor defects. AlN defects act as scattering centers and cause low mobility.

The ZnO:Al:N thin films grow with a *c*-axis preferential orientation and the (002) diffraction line has maximum intensity independently of the substrate temperature or the dopant concentration. They exhibit high visible transparency of about 90%. A decrease in optical band gap at co-doped *p*-type ZnO was observed (Ge et al., 2004).

### 3. Development and characterization of nitrogen-doped and aluminium-nitrogen co-doped ZnO thin films: Results and discussions

Our previous studies on un-doped ZnO films (chemo-resistive films for gas sensing and piezoelectric high resistive films for SAW sensors and micro-actuators), laid the groundwork for current experiments (Tvarozek et al., 2007). The experiments of Yao et al., mentioned in the previous part (Yao et al., 2007), provided evidence of successful *p*-doping using  $\text{N}_2$  source. Co-doping simultaneously with nitrogen and group III element should be a more effective strategy to achieve a low resistivity *p*-type ZnO material than nitrogen mono-doping (Yamamoto, 2002). This concept was verified by many research groups and discussed in the co-doping section of this chapter. In the following subsections we shall describe our experimental results and shall discuss the effects of nitrogen doping and aluminum - nitrogen co-doping on structural and electrical properties of ZnO thin films

prepared by RF diode sputtering. Moreover, structural and electrical features of ZnO films grown on both Corning glass and Si/SiO<sub>2</sub> substrate under the same and different growth conditions will be compared.

### 3.1 Thin films deposition

The nitrogen-doped and the aluminum - nitrogen co-doped (ZnO:Al:N) thin films, discussed in this chapter, were deposited in a planar radio frequency (RF) sputtering diode system Perkin Elmer 2400/8L. Using of RF sputtering in reactive plasma is a new approach to preparation of ZnO thin films of required properties. In RF diode sputtering a flux of charged and neutral particles interacts with the growing film. This energetic particles bombardment increases the substrate/film temperature ( $T_s$ ) and reduces the formation energy of the nitrogen acceptor providing conditions for effective *p*-type doping of the ZnO thin films. The total energy density ( $E_\phi$ ) of the flux significantly affects and modifies the crystalline structure and hence the electrical and the optical properties of the RF sputtered ZnO thin films. The N<sub>2</sub> dopant source, chosen among the other nitrogen sources, is an easy getting, economic lucrative and non-toxic. The ZnO:N thin films were deposited on Corning glass substrates or on n-type Si (100) wafers covered by thermal Si oxide of thickness 0.8  $\mu\text{m}$ , from a ZnO ceramic target (purity 99.99%), in Ar/N<sub>2</sub> working gases. The diameter of the ZnO target was 203.2 mm. A sintered ceramic target ZnO:Al<sub>2</sub>O<sub>3</sub> (98wt%:2wt%), a mixture of ZnO (purity 99.99%) and Al<sub>2</sub>O<sub>3</sub> (purity 99.99%), in diameter 152.4 mm, was used for the deposition of ZnO:Al:N films. They were deposited on Corning glass substrates in Ar/N<sub>2</sub> working gases. In both cases, the vacuum chamber was evacuated to a base pressure of  $2 \times 10^{-5}$  Pa before admission of gases of purity: Ar (99.999%) and N<sub>2</sub> (99.999%). The working gas pressure of 1.3 Pa and the sputtering power (500 W for ZnO:N and of 417 W for ZnO:Al:N films), were maintained constant during deposition. Varying deposition parameters were percentage of nitrogen (0 % ÷ 100 %) in the sputtering gas, and the bias voltage applied on the substrate (-25 V, -50 V and -100 V). Depending on the deposition time that varies from 30 to 60 minutes, the thickness of the ZnO films ranged from 430 nm to 870 nm. The film thickness was evaluated by a Talystep instrument. The substrate temperature  $T_s$  = room temperature and the ratio  $E_\phi / E_{\phi_{min}} \geq 7$ .

### 3.2 Micro structural parameters of nitrogen-doped and Al:N<sub>2</sub> co-doped ZnO thin films

X-ray diffraction provides general purpose qualitative and quantitative information on the composition and structure of the studied material and was used for qualitative structure analysis of nitrogen mono-doped and Al:N<sub>2</sub> co-doped ZnO films. Diffraction line contains a lot of information of which four parameters are of special interest: (i) peak position, (ii) FWHM (full width at half maximum), (iii) intensity of its maximum and (iiii) integrated intensity (area below the diffraction line). These parameters were used to identify the contents of the sample, as well as to evaluate important material parameters such as crystallite size ( $D$ ), crystallinity, stress and strain ( $\langle \epsilon \rangle$ ).

X-ray diffraction patterns of the ZnO:N thin films were recorded on an AXS Bruker D8 powder diffractometer (symmetric  $\Theta$  - $2\Theta$  geometry and pseudo-parallel beam), equipped by 2D detector and an Eulerian cradle. CoK $\alpha$  radiation ( $\lambda = 0.179$  nm) was used. A method proposed by Langford, based on the X-ray diffraction line profile analysis, was used to perform the size-strain analysis (micro-strains and crystallite sizes).

The microstructure of ZnO:Al:N thin films was analyzed on a thin film attachment (asymmetric  $\omega$ - $2\theta$  geometry and pseudo-parallel beam) and on an X'pert Pro powder diffractometer at a constant incident angle  $\omega$  of  $1^\circ$  with an observation  $2\theta$  range from 20 to  $40^\circ$ . Cu  $K\alpha$  ( $\lambda = 0,154$  nm) radiation was used. In both cases, a ceramic alumina from NIST (National Institute of Standards and Technology) was used as an instrumental standard (Fig. 2).

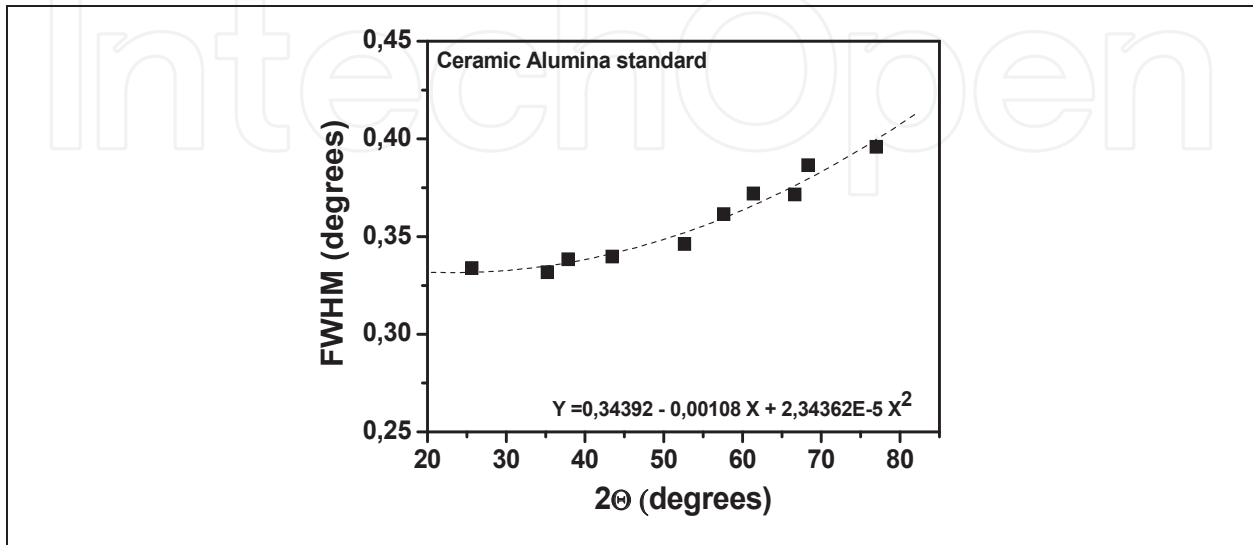


Fig. 2. Dependence of FWHM of Ceramic Alumina standard on  $2\theta$

The diffraction indices for the crystal planes of pure ZnO, their  $2\theta$  (Cu $K\alpha$ ) values, d-spacings and relative intensities calculated by APX 63 - Struc software are presented in Table 4.

Plane (hkl)	d-Spacing (nm)	$2\theta$ ( $^\circ$ )	Relative Intensity (%)
(100)	0.281450	37.088	48
(002)	0.260330	40.221	36
(101)	0.247591	42.388	100
(110)	0.162495	66.851	28
(103)	0.147725	74.591	30
(004)	0.130165	86.892	2

Table 4. XRD reference data for hexagonal ZnO calculated by using APX 63 - Struc software (Kraus, I., 1993)

### 3.2.1 ZnO:N thin films

Structural parameters of ZnO:N films, deposited on Corning glass and Si/SiO<sub>2</sub> substrates, were examined as a function of two deposition variables: the N<sub>2</sub> content in the working gas and the negative bias voltage applied on the substrate (Table 5). It was found out that both variables influence the film crystalline quality.

The XRD patterns presented in Fig. 3, from the observed range ( $30^\circ < 2\theta < 80^\circ$ ), show the diffraction lines of ZnO:N thin films deposited on Corning glass 7059 substrates. The plots show the results for a different content of N<sub>2</sub> in the sputtering gas under 0 V bias.

N <sub>2</sub> content (%)	Mode	Substrate	D (nm)	< $\epsilon$ > (-)
0	sputter	Corning 7059	37	1.0x10 <sup>-2</sup>
10	sputter	Corning 7059	140	1.6x10 <sup>-2</sup>
25	sputter	Corning 7059	20	1.6x10 <sup>-2</sup>
50	sputter	Corning 7059	12	1.3x10 <sup>-2</sup>
75	sputter	Corning 7059	8	1.2x10 <sup>-2</sup>
100	sputter	Corning 7059	24	1.2x10 <sup>-2</sup>
75	bias -25 V	Corning 7059	11	1.26x10 <sup>-2</sup>
75	bias -50 V	Corning 7059	11	0.75x10 <sup>-2</sup>
25	sputter	Si/SiO <sub>2</sub>	12	9.57x10 <sup>-3</sup>
50	sputter	Si/SiO <sub>2</sub>	-	-
75	sputter	Si/SiO <sub>2</sub>	37	13.2x10 <sup>-3</sup>

Table 5. Crystallite size and strain as a function of nitrogen percentage in the working gas and the negative bias voltage

Three dominant lines (100), (002), and (101) appear in the XRD patterns of all ZnO films. The fourth diffraction line (110), is available only in the patterns of the films deposited at 25, 50 and 75 % N<sub>2</sub> in the sputtering gas. The XRD patterns clearly show the change in the growth direction with increasing nitrogen content. A strong (002) line at  $2\theta \sim 40^\circ$ , and weak (100) and (101) features at  $2\theta \sim 36.9^\circ$ ,  $42^\circ$ , for un-doped (0 % N<sub>2</sub>) films and those grown with 10 and 100 % N<sub>2</sub>, provide evidence for their polycrystalline hexagonal structure with a preferential c-axis orientation, perpendicular to the substrate. As nitrogen content increases (25, 50 and 75 %), the (002) peak intensity decreases while its full width at half maximum (FWHM) increases. The diffraction lines corresponding to (100), (101) and (110) crystal planes rise, showing that the ZnO:N thin films become more randomly orientated.

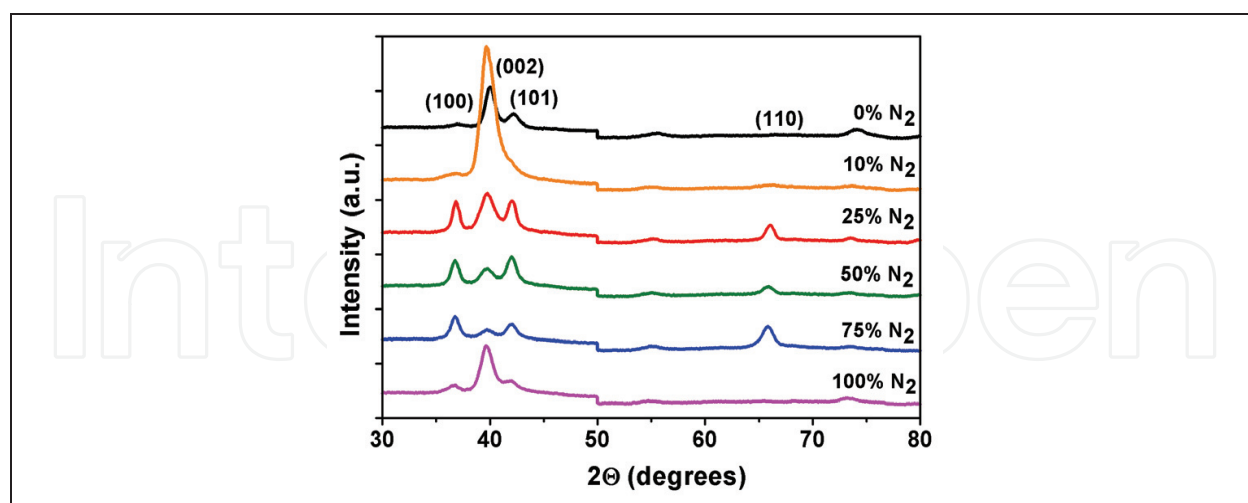


Fig. 3. X-ray diffraction patterns of ZnO:N deposited on Corning glass 7059 substrates as a function of nitrogen percentage in the working gas

The  $2\theta$  diffraction angle values are slightly smaller than the standard values given in Table 4 for all three dominant lines (100), (002), and (101) respectively. Depending on N<sub>2</sub> content, their position shifts  $0.2^\circ$  to  $0.6^\circ$  lower for nitrogen-doped ZnO films compared to the standard values (Table 4) for un-doped ZnO. This shift can be explained by compressive

lattice strains (stresses) created during sputtering process and can be quantitatively evaluated from the equation for biaxial lattice stress (Šutta & Jackuliak, 1998)

$$\sigma_1 + \sigma_2 = -\frac{E}{\mu} \cdot \frac{d - d_0}{d_0} \quad (1)$$

where  $E$  is Young's modulus,  $\mu$  is Poisson's ratio,  $d_0$  is the reference strain-free interplanar spacing and  $d$  is the interplanar spacing obtained from the experiment. According the Bragg law the decrease of the diffraction angle with increasing  $N_2$  content will increase the interplanar spacing  $d$  thus introducing stress into the film. Therefore, the shift of the position of (002) line toward the lower angles is an indicator of tensile stress in the ZnO thin films.

The estimated crystallite size ranges from 8 to 140 nm with varying  $N_2$  content in working gas. Crystallite size is a measure of the size of a coherently diffracting domain and can be estimated using a Scherrer's formula:

$$\langle D \rangle = \frac{K\lambda}{\beta_C^f \cos\Theta} \quad (2)$$

where  $K = 2\sqrt{\ln 2/\pi} \approx 0.94$  is the Scherrer's constant,  $\lambda$  is the wavelength of the X-rays used,  $\beta_C^f$  is the pure (physical) Cauchy component of integral breadth of the line taken in radians and  $\Theta$  is the Bragg's angle (Delhez et al., 1982). Average micro-strain is about  $1 \times 10^{-2}$  and was determined using the equation:

$$\langle \varepsilon \rangle = \frac{\beta_G^f}{4\text{tg}\Theta} \quad (3)$$

where  $\beta_G^f$  is the pure (physical) Gaussian component of integral breadth of the line taken in radians (Delhez et al., 1982). Some researchers have interpreted the strain in nitrogen-doped thin films and structural deformations in terms of the increase of complex defect density in the material (Park et al., 2008). It was observed that ZnO:N films grown at low temperatures ( $< 500^\circ\text{C}$ ), suffer from high residual tensile stress. One reason for this stress can be the effect of the film thickness and the other is the incorporation of nitrogen. Since Zn-N bond length (2.04 Å) is somehow longer than the length of Zn-O bond (1.93 Å), it is expected that nitrogen incorporation will cause lattice expansion.

It is commonly accepted that substrate temperature has a significant effect on physical properties of the film. Since a negative bias voltage applied on the substrate causes an intensive positive ions bombardment on the substrate, it will increase the substrate temperature. The XRD patterns for ZnO:N thin films deposited at three different negative bias voltages, 0, -25 and -50 V, applied on the substrate, and at a constant  $N_2$  content of 75%, are displayed on a Fig. 4. The crystalline structure of the ZnO:N thin films deposited without bias and at bias voltage of -25 V is random orientated with a dominant (100) feature at  $2\Theta \sim 36.7^\circ$ , while that of the films deposited at -50 V bias gives well defined (002) diffraction line at  $2\Theta \sim 39.7^\circ$  and two weaker (100) and (101) diffraction lines, indicating preferential orientation growth. The narrowing of the (002) and the widening of (100) and (101) diffraction lines are clear observable. The  $2\Theta$  diffraction angle positions remain uninfluenced from the negative bias voltage. The crystallite size and average microstrain are slightly influenced from the increase of the bias voltage.

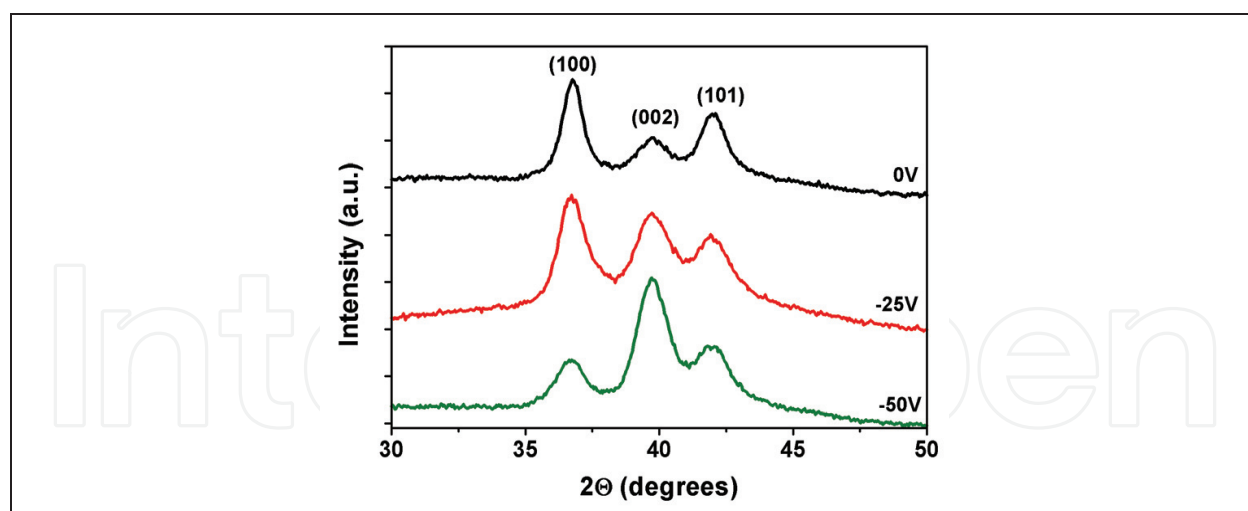


Fig. 4. XRD patterns of ZnO:N thin films deposited on Corning glass 7059 substrates at 75 %  $N_2$  content as a function of the bias voltages

The XRD patterns presented in Fig. 5, recorded for  $30^\circ < 2\theta < 80^\circ$ , show the diffraction lines for ZnO:N thin films deposited on Si/SiO<sub>2</sub> substrates at different contents of  $N_2$  in the sputtering gas. The XRD patterns reveal four dominant lines at  $2\theta$  diffraction angles of approximately  $36.2^\circ$ ,  $39.4^\circ$ ,  $41.46^\circ$ , and  $65.6^\circ$ , which correspond to (100), (002), (101), and (110) planes of the hexagonal ZnO structure respectively.

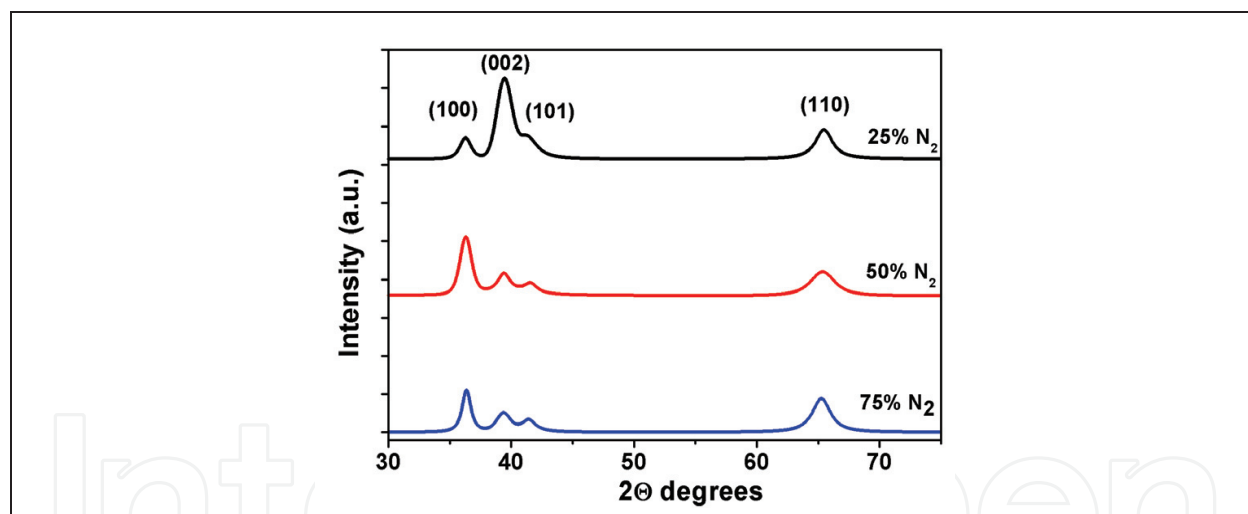


Fig. 5. X-ray diffraction patterns of ZnO:N deposited on Si/SiO<sub>2</sub> substrates as a function of nitrogen percentage in the working gas

Diffraction lines from (103) and (004) crystal planes listed in Table 4 are missing, and the intensities from detected lines do not match the listed relative intensities. In fact, the variation tendencies in the diffraction angle positions and the intensities with  $N_2$  content are the same as for the films deposited on a glass substrate.

The dominant (002) diffraction line of ZnO thin films deposited at 25 %  $N_2$  in the sputtering gas indicates a good crystalline quality with a preferential c-axis orientation, perpendicular to the substrate. As nitrogen percentage in the working gas increases (50 %, 75 %  $N_2$ ), the intensity of (002) line decreases and its width increases. In parallel, the rise of (100) and (101) diffraction lines is observed indicating that the crystallites become randomly orientated.

The  $2\theta$  diffraction angles are smaller than the standard values given in a table 4 for all four dominant lines (100), (002), (101), and (110) respectively. They shift from  $0.8^\circ$  to  $1^\circ$  lower in ZnO:N compared to the standard values (Table 4) for un-doped ZnO.

The grain size (12 to 37 nm) increases and average microstrains decrease ( $0.97 \times 10^{-2}$  to  $1.32 \times 10^{-2}$ ) with increasing  $N_2$  content in the sputtering gas.

XRD patterns of ZnO:N deposited at 75 %  $N_2$  on Si/SiO<sub>2</sub> and Corning glass 7059 substrates are compared in Fig. 6.

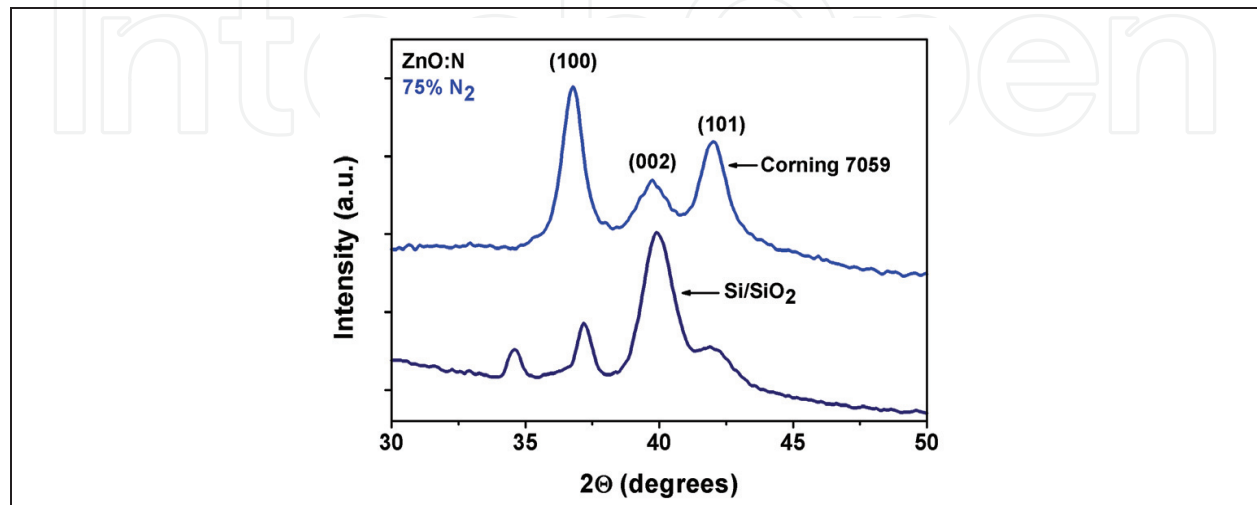


Fig. 6. X-ray diffraction patterns of ZnO:N deposited on Corning glass 7059 and Si/SiO<sub>2</sub> substrates at 75 %  $N_2$  content in the working gas

### 3.2.2 ZnO:Al:N thin films

Structural properties of aluminum-nitrogen co-doped ZnO films, sputtered on Corning glass substrate were investigated as a function of nitrogen percentage in the sputtering Ar/ $N_2$  gas mixture. X-ray diffraction show that co-doping improves the crystalline structure and all ZnO:Al:N thin films show a c-axis texture in direction declined about 16 deg from the surface normal. The XRD patterns of ZnO:Al:N thin films deposited at four nitrogen contents (0, 25, 50 and 75 %  $N_2$ ), are recorded for  $30^\circ < 2\theta < 50^\circ$  (Fig. 7). They reveal more or

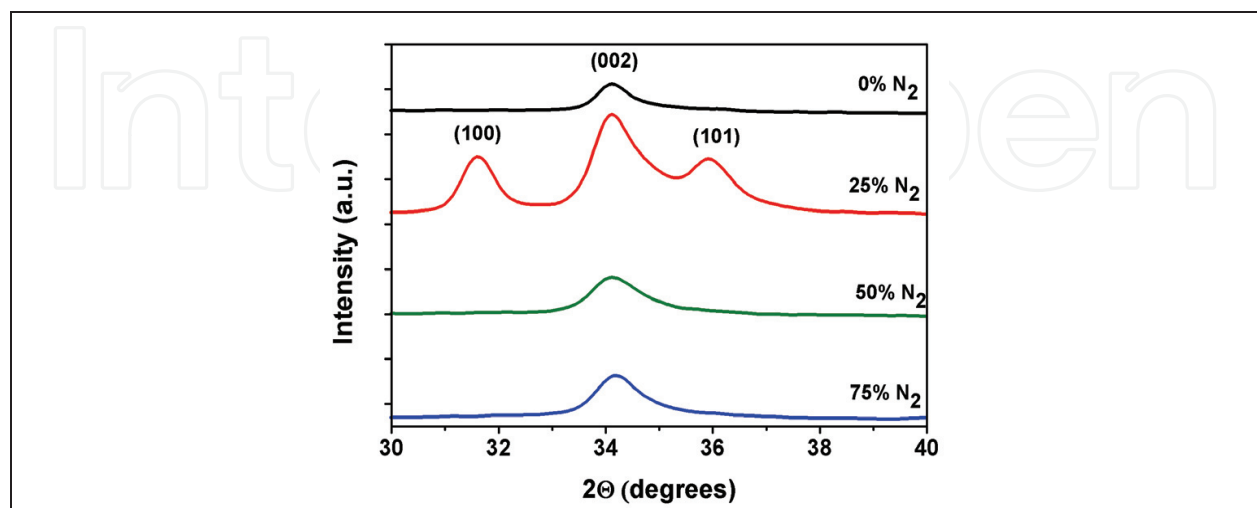


Fig. 7. X-ray diffraction patterns of ZnO:Al:N deposited on Corning glass 7059 substrates as a function of nitrogen percentage in the working gas

less stronger expressed c-axis preferential orientation of the films depending on the N<sub>2</sub> content in the sputtering gas. (100), (002) and (101) diffraction lines appear in the XRD patterns of the films deposited at 25 % N<sub>2</sub>, indicating that their preferential orientation is more random. A strong preferential orientation of the crystallites is observed for high dopant contents (50 % and 75 % N<sub>2</sub>) and the intensities of the (002) diffraction lines are almost the same. The diffraction lines are asymmetric more likely due to the incorporation of the Al and the formation of different phases (AlO) at the interface, which causes broadening of the line toward the higher diffraction angles. The estimated grain size changes from 21 to 33 nm and microstrains vary from 4.5x10<sup>-3</sup> to 9.6x10<sup>-3</sup> with the N<sub>2</sub> content.

### 3.3 Electrical characterization of doped and co-doped ZnO thin films

Hall-effect measurements are widely used technique to determine the electrical properties, and to evaluate the quality of the semiconductor materials. This technique allows to measure directly the carrier type and concentration. Other attractive properties, which make this characterization technique so popular, are its cost, simplicity and ease of use, although a special sample geometry is required and measurement is sensitive to the contact. Contemporary semiconductor physics acknowledges carrier concentration ( $n/p$ ) and carrier mobility ( $\mu_n/\mu_p$ ), fundamental electrical parameters, while resistivity is related to those two parameters. The Hall coefficient ( $R_H$ ) and resistivity ( $\rho$ ), are determined experimentally. The hole concentration is a function of the Hall constant and is given by

$$p = \frac{1}{qR_H} \quad (4)$$

Similarly for an  $n$ -type semiconductor

$$n = -\frac{1}{qR_H} \quad (5)$$

For known resistivity  $\rho$ , the carrier drift mobility is evaluated using the formula:

$$\mu = \frac{|R_H|}{\rho} \quad (6)$$

The Hall-effect measurements of ZnO:N and ZnO:Al:N thin films were carried out at room temperature (RT). The measured samples have geometry of a 1x1 cm square. The ohmic contacts were made by small indium dots at the four corners of square samples, so that, their average diameter and also the film thickness were significantly smaller than the distance between the contacts. In order to exclude photoconductive and photovoltaic effects the samples were measured in the dark. The Hall system was assembled from a Tesla Multimeter model BM518, a voltage source Statron model 3205 covering the voltage range from 0 to 30 V and a high input impedance voltmeter. The magnetic field of 0.385 T was created from a permanent magnet. The obtained measurement results were acquired and processed by a personal computer (PC) and home developed software. The data reported from PC were a carrier type and concentration  $p/n$ , resistivity  $\rho$ , Hall coefficient  $R_H$  and carrier (or Hall) mobility  $\mu_H$ . When evaluating the Hall measurement results should be

considered some underlying limits associated with them like are Hall scattering factor ( $r_H$ ) (generally assumed to be 1), and the small magnitude of the Hall voltage. For thin films with low Hall mobility like ZnO:N and ZnO:Al:N the difference between the Hall voltage with and without a magnetic field will be small, making accurate measurement of the Hall voltage difficult. This required repeating and careful measurements to make sure the measured changes in the Hall voltage were accurate and consistent for the applied magnetic field and current.

### 3.3.1 ZnO:N thin films

The room temperature Hall measurements were carried at specified currents, depending on the film's resistivity. Four types of variations are followed in the data depending on the N<sub>2</sub> content in the sputtering gas, negative bias voltage on the substrate, type of the substrate and heat treatment.

#### 3.3.1.1 Effect of the N<sub>2</sub> content in the sputtering gas

The electrical parameters of ZnO:N deposited on Corning Glass substrates as a function of the N<sub>2</sub> content into the sputtering gas are specified in Table 6.

N <sub>2</sub> content (%)	Mobility (cm <sup>2</sup> /Vs)	Concentration (cm <sup>-3</sup> )	Resistivity (Ωcm)
0	NM	NM	NM
10	NM	NM	5.4x10 <sup>4</sup>
25	3	$p \sim 1.2 \times 10^{15}$	1.5x10 <sup>3</sup>
50	23	$n \sim 4 \times 10^{14}$	7.0x10 <sup>2</sup>
75	25	$p \sim 3.2 \times 10^{14}$	7.9x10 <sup>2</sup>
100	23	$p \sim 1.3 \times 10^{14}$	2.1x10 <sup>3</sup>

Table 6. Electrical parameters of ZnO:N deposited on Corning glass 7059 substrates as a function of the N<sub>2</sub> content

The term NM refers to "not measurable", when the sample's resistance is too high (higher than 5.4x10<sup>4</sup> Ωcm) and the current source is unable to drive the necessary current. This occurred for ZnO:N thin films deposited without N<sub>2</sub> and with 10 % N<sub>2</sub> in the sputtering gas. The effect of the N<sub>2</sub> content on the resistivity, mobility and carrier concentration of *p*-type ZnO:N thin films grown on Corning glass substrates can be seen in Fig. 8. The resistivity of the un-doped ZnO thin films (0 % N<sub>2</sub> in the sputtering gas) is too high to be measured. In fact, the films doped at 10 % N<sub>2</sub> have the highest resistivity of 5.4x10<sup>4</sup> Ωcm.

Owing to nitrogen incorporation and creation of nitrogen acceptors, the films prepared at 25 %, 75 % and 100 % N<sub>2</sub> in the sputtering gas show *p*-type features. Nitrogen incorporation was confirmed by secondary ion mass spectroscopy (SIMS) (Shtereva et al., 2006).

Conductivity type of the samples grown at 50% nitrogen is rather controversial and statistically was determined to be *n*-type. Four subsequent measurements were conducted with a current of 200 nA driven through this sample. With the measured Hall voltages, film's thickness and current, type of conductivity was determined three times as *n*-type, and once as *p*-type. Measurement was repeated and three subsequent measurements were carried out with a current of 500 nA. The calculations with newly obtained Hall voltages determined the sample two times as a *p*-type and once as an *n*-type. Since denoted *n*-type, the electrical parameters of this sample are not included in Fig. 8 and the following discussion.

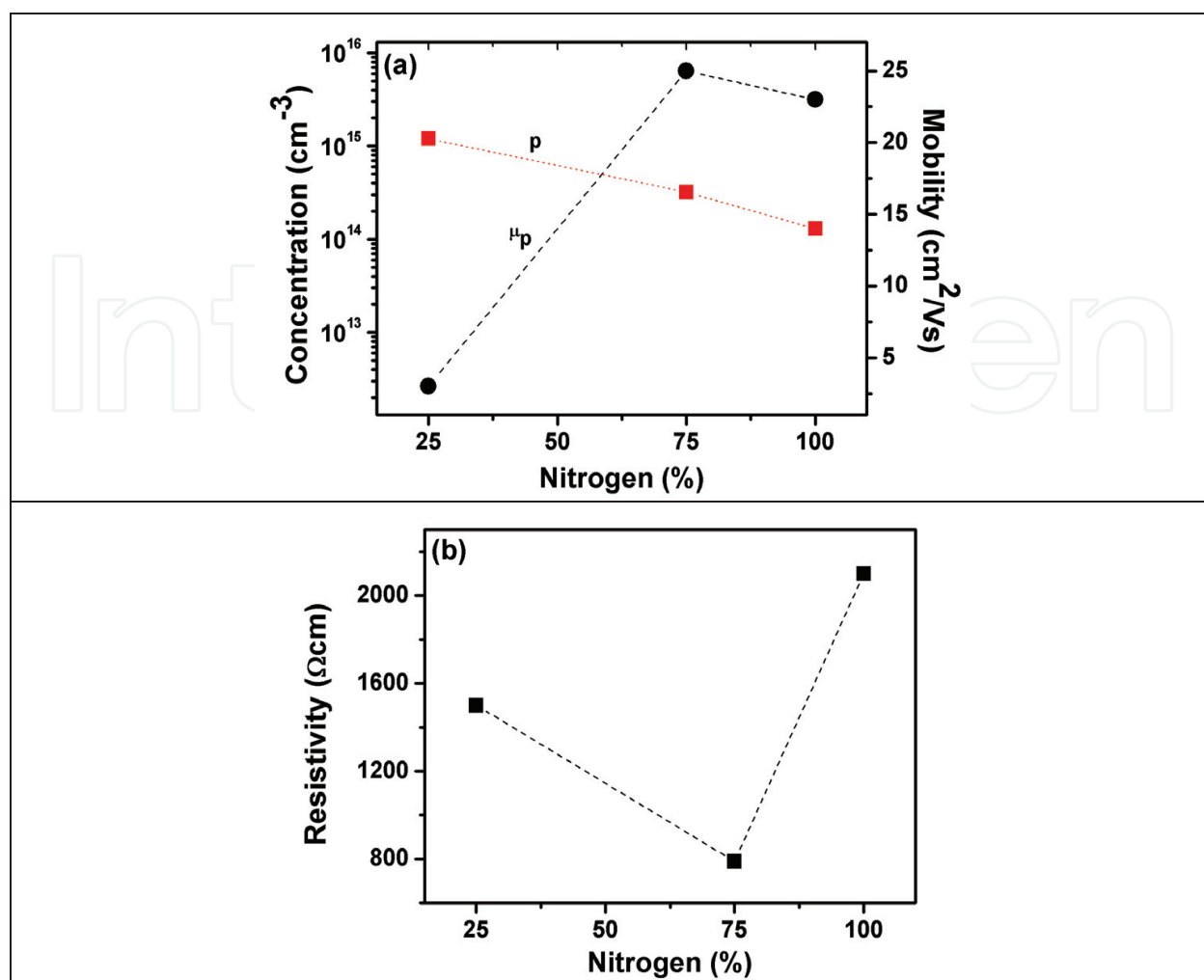


Fig. 8. Effect of the N<sub>2</sub> content on (a) the carrier concentration and mobility, and (b) resistivity for ZnO:N deposited on Corning glass 7059 substrates

Resistivity variations of two orders of magnitude, mobility variations of a factor of  $\sim 8$ , and concentration variations of an order of magnitude occur with N<sub>2</sub> content changing from 25 to 100%. More than 50% reduction of the resistivity, from  $1.5 \times 10^3 \Omega\text{cm}$  to  $7.9 \times 10^2 \Omega\text{cm}$ , follows the increase of nitrogen percentage from 25 to 50%. The lowest resistivity is obtained for 75% N<sub>2</sub> and is a result of the highest mobility. The further supply of nitrogen to the Ar/N<sub>2</sub> gas to amount of 100%, leads to 2.7 times increase of the resistivity to the value of  $2.1 \times 10^3 \Omega\text{cm}$ .

Although the SIMS depth profile shows the incorporation of nitrogen in the films, the carrier concentration is reduced from  $1.2 \times 10^{15} \text{cm}^{-3}$  to  $1.3 \times 10^{14} \text{cm}^{-3}$  when nitrogen percentage in working gas increasing from 25 to 100%. The reason for this decrease in the carrier concentration is more likely due to compensation of the N<sub>O</sub> acceptor by native and nitrogen related donor defects as well as by unintentionally introduced donor defects. First-principals calculations denote O vacancies and N-acceptor - Zn-antisite (N<sub>O</sub>-Zn<sub>O</sub>) complexes major compensating donors for a normal N<sub>2</sub> source, whereas nitrogen molecules (N<sub>2</sub>)<sub>O</sub> and N<sub>O</sub> - (N<sub>2</sub>)<sub>O</sub> complexes are the major compensating species for a plasma N<sub>2</sub> source (Lee et al, 2001). Hence, achievement of high hole concentrations at low nitrogen doping levels is restricted by the O vacancies, whereas at high doping levels the N<sub>O</sub> acceptor is compensated by donor complexes that nitrogen forms with the native defects. More recent theoretical

results point to the role of the complexes that nitrogen acceptor forms with unintentionally introduced donor defects, such as hydrogen ( $\text{N}_\text{O} - \text{H}$  complex with a low binding energy of about 1 eV), and the carbon impurities ( $\text{NC}_\text{O}$  and  $(\text{N}_2)_\text{O}$ ) (Limpijumnong et al., 2006). They both are donors and compensate the  $\text{N}_\text{O}$  acceptor. N and C were registered by SIMS in all our ZnO:N films.

Chemical potential for nitrogen ( $\mu_\text{N}$ ) increases and the activation energy of the  $\text{N}_\text{O}$  acceptor decreases as a result of the increase in N concentration. Chemical potential for nitrogen is determined by the formation energy of the nitrogen molecule ( $\mu_\text{N}^\text{max} = \frac{1}{2} \mu_{\text{N}_2}$ ), hence, the formation energy of  $(\text{N}_2)_\text{O}$  molecule decreases double, which means that in thermal equilibrium conditions the concentration of  $(\text{N}_2)_\text{O}$  donors will increase faster than the concentration of acceptors (Zhang et al., 2001). This explains why the increase in the N concentration often does not result in high hole concentrations p-type ZnO.

The carrier transport is influenced from various scattering mechanisms that determine carrier mobility in semiconductors. The major scattering mechanisms in ZnO thin films are presumed to be: (i) ionized impurity scattering; (ii) neutral impurity scattering, and (iii) grain boundary scattering. In the case of ionized impurity scattering, mobility shall decrease with increasing carrier concentration when the free carriers' density is equal to the concentration of the ionized donors/acceptors. The dependence of mobility on carrier concentration is plotted on Fig. 9. Mobility increases with increasing  $\text{N}_2$  content from 25 to 75 % in consequence of the decreasing hole concentration (Fig. 8a). The highest Hall mobility of  $25 \text{ cm}^2/\text{Vs}$  along with a hole concentration of  $3.2 \times 10^{14} \text{ cm}^{-3}$  are found in ZnO:N prepared at 75 %  $\text{N}_2$  and result in the lowest resistivity of these films.

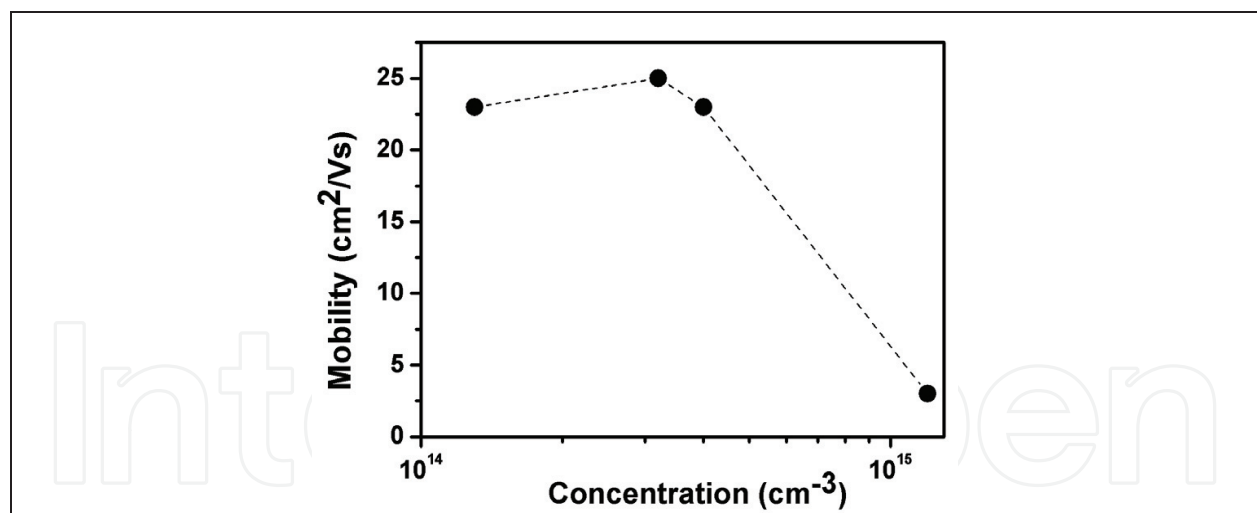


Fig. 9. Mobility of ZnO:N films as a function of the carrier concentration

### 3.3.1.2 Effect of the negative bias voltage applied on the substrate

The electrical parameters of ZnO:N thin films deposited on Corning Glass and Si/SiO<sub>2</sub> substrates as a function of the negative bias voltage applied on the substrate are given in Table 7. All films were prepared at 75 %  $\text{N}_2$  in the sputtering gas.

Fig. 10 illustrates how the hole carrier concentration, resistivity and mobility vary with the negative bias voltage for ZnO:N films deposited on glass substrates. Irrespectively of the used substrate, the carrier concentration is lower, and mobility and resistivity are higher, for samples prepared at negative bias compared to those grown without a bias voltage. Indeed,

Substrate	Bias voltage (V)	Mobility (cm <sup>2</sup> /Vs)	Concentration (cm <sup>-3</sup> )	Resistivity (Ωcm)
Si/SiO <sub>2</sub>	0	469	$p \sim 2.0 \times 10^{12}$	$6.7 \times 10^3$
Si/SiO <sub>2</sub>	-25	371	$p \sim 2.6 \times 10^{12}$	$6.4 \times 10^3$
Si/SiO <sub>2</sub>	-50	480	$n \sim 1.7 \times 10^{12}$	$7.7 \times 10^3$
Si/SiO <sub>2</sub>	-100	28	$p \sim 4.0 \times 10^{13}$	$5.7 \times 10^3$
Glass	0	25	$p \sim 3.2 \times 10^{14}$	$7.9 \times 10^2$
Glass	-25	121	$p \sim 1.2 \times 10^{13}$	$4.4 \times 10^3$
Glass	-50	51	$p \sim 2.6 \times 10^{13}$	$4.7 \times 10^3$
Glass	-100	357	$n \sim 5.0 \times 10^{12}$	$3.5 \times 10^3$

Table 7. Electrical parameters of ZnO:N deposited on Corning glass 7059 and Si/SiO<sub>2</sub> substrates as a function of the negative bias voltage

the intensive bombardment by positive ions on the substrate, induced from the negative bias voltage, will increase the substrate temperature and hence, improvement of the crystalline structure of the film discussed in the previous subsection. On the other hand, this ion bombardment can induce defects in the film, which influence its electrical parameters.

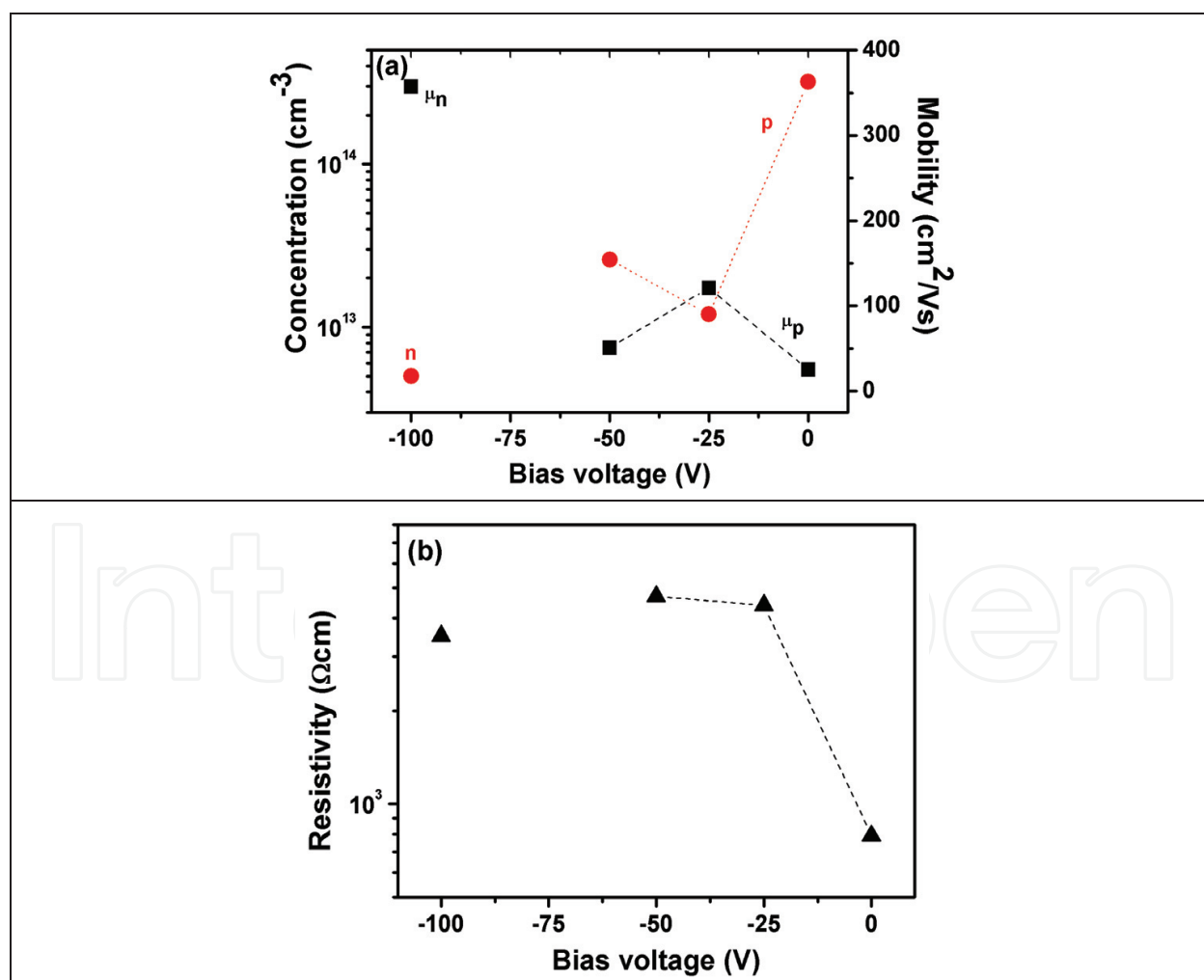


Fig. 10. Effect of the bias voltage on (a) the carrier concentration and mobility and (b) resistivity, for ZnO:N deposited on Corning glass 7059 substrates

### 3.3.1.3 Effect of annealing

Post-deposition annealing is known to improve crystalline structure and to decrease the background defects in ZnO. The ZnO:N thin films deposited with 75 % and 100 % N<sub>2</sub> in the sputtering gas (Samples No 12 and 13) were annealed in N<sub>2</sub> atmosphere at a temperature of 600°C for 10 minutes. The electrical parameters of the as deposited and annealed samples are presented in a Table 8.

Sample Noe	N <sub>2</sub> content (%)	Mobility (cm <sup>2</sup> /Vs)	Concentration (cm <sup>-3</sup> )	Resistivity (Ωcm)
12	75	25	p~ 3.2x10 <sup>14</sup>	7.9x10 <sup>2</sup>
13	100	23	p~ 1.3x10 <sup>14</sup>	2.1x10 <sup>3</sup>
12A	75	5	n~ 5.4x10 <sup>18</sup>	2.4
13A	100	3	n~ 1.1x10 <sup>18</sup>	2

Table 8. Electrical parameters of ZnO:N thin films as a function of annealing in N<sub>2</sub> atmosphere at temperature of 600°C.

The annealed samples are marked as 12A and 13A respectively.

After annealing, type of conductivity changes from *p*-type to *n*-type for both samples more likely due to the out-diffusion of nitrogen from the film during heat treatment and the decrease in concentration of the nitrogen acceptors. Mobility and resistivity are reduced as a result of the increase carrier concentration.

Raman spectra of ZnO:N films reveal a decrease in intensity of the peak at 271.5 cm<sup>-1</sup> that is assigned to the local vibrational modes (LVM) of nitrogen (Tvarozek et al. 2008). According to some works, intensity of the dopant's LVM has a linear dependence on the dopant concentration (Kaschner et al. 1999). On the other hand, intensity of the peak at 576.7 cm<sup>-1</sup>, which is associated with the presence of defects, such as O vacancies and Zn interstitials, increases after annealing.

### 3.3.2 ZnO:Al:N thin films

The aim of these experiments was to investigate the influence of Al - N<sub>2</sub> co-doping on the electrical properties of sputtered ZnO thin films and thereby to verify the effectiveness of the co-doping concept. The importance of this task is determined by the following requirements: (i) to decrease their resistivity and increase their transmittance and (ii) to understand better the role of aluminum, as nitrogen co-dopant, on their physical properties. The ZnO:Al:N thin films were deposited at different N<sub>2</sub> contents in the sputtering gas mixture: 0 %, 25 %, 50 % and 75 %. Their electrical parameters were determined by means of Hall-effect measurements, carried out at room temperature. In contrary to ZnO:N, the Al - N<sub>2</sub> co - doped thin films have lower resistivity which allowed the Hall voltages to be taken at higher currents, depending on the film resistivity. Hall data, taken twice with two weeks period between the first and the second measurement, are listed in Table 9.

As expected, the thin films doped only with aluminum, without nitrogen in the sputtering gas (ZnO:Al), are *n*-type and high conductive. The high carrier concentrations of ZnO:Al compared to nitrogen-doped ZnO results from the contribution of the Al<sup>3+</sup> substituents in addition to the native donor defects.

The conductivity type of the samples prepared with 25 % N<sub>2</sub> in the sputtering gas was unstable, being *p*-type during the first measurement and turning to *n*-type during the

N <sub>2</sub> content (%)	Mobility (cm <sup>2</sup> /Vs)	Concentration (cm <sup>-3</sup> )	Resistivity (Ωcm)
0	1	n ~ 5.1x10 <sup>19</sup>	8.9x10 <sup>-2</sup>
25	4	n ~ 1.1x10 <sup>18</sup>	1.5
50	2	n ~ 6.5x10 <sup>17</sup>	6.1
75	0.4	p ~ 7.8x10 <sup>17</sup>	21

Table 9. Electrical parameters of ZnO:Al:N deposited on Corning glass 7059 substrates as a function of the N<sub>2</sub> content

second measurement, which is an indication of a compensate semiconductor. The films prepared at 50% N<sub>2</sub> exhibit persistent *n*-type conductivity. These results are consistent with the results obtained for nitrogen mono-doped ZnO and discussed in the previous subsection.

The repeated measurements show a stable *p*-type features of the ZnO:Al:N thin films prepared at 75 % N<sub>2</sub> in the sputtering gas. It suggests existence of the “nitrogen content window” where *p*-type doping in ZnO can be realized. The resistivity of *p*-type ZnO:Al:N thin films measured in this experiment is 21 Ωcm, which is roughly a factor of 40 lower than the lowest ZnO:N resistivity (790 Ωcm), reported in 3.3.1.1. Accordingly, the hole carrier concentration of the former (7.8x10<sup>17</sup> cm<sup>-3</sup>) is more than three orders of magnitude higher than the ZnO:N hole concentration (3.2x10<sup>14</sup> cm<sup>-3</sup>). This electrical parameters improvement is due to Al co-doping.

The carrier concentration, resistivity and Hall mobility are plotted as a function of the N<sub>2</sub> content in Fig. 11.

#### 4. Conclusions

Our research on the growing and characterizing of *p*-type ZnO thin films, prepared by radio frequency (RF) diode sputtering, mono-doped with nitrogen, and co-doped with aluminium and nitrogen, is a response of the need from *p*-type ZnO thin films for device applications. The dopants determine the conductivity type of the film and its physical properties. We obtained *p*-type ZnO thin films by RF diode sputtering and using a nitrogen dopant source. The novelty in our approach is in the use of a plasma assisted deposition method, to increase nitrogen solubility and the concentration of the N<sub>O</sub> acceptors in the film.

The structural parameters, such as preferential orientation, crystallite size and strain in the film, depend on percentage of nitrogen in the working gas and the negative bias voltage. The XRD diffraction patterns reveal more or less stronger expressed *c*-axis preferential orientation of the films depending on the N<sub>2</sub> content in the sputtering gas. The diffraction lines of ZnO (100), (002), (101), and (110) are observed in the XRD diffraction patterns of all ZnO:N thin film. Aluminium- nitrogen co-doping improves the crystalline structure and all ZnO:Al:N thin films show a *c*-axis texture in direction declined about 16 deg from the surface normal. Three diffraction lines ((100), (002) and (101)), appear only in the XRD patterns of the films deposited at 25 % N<sub>2</sub>, indicating that their preferential orientation is more random. A strong preferential orientation of the crystallites is observed for high dopant contents (50 % and 75 % N<sub>2</sub>) and intensities of the (002) diffraction lines are almost the same.

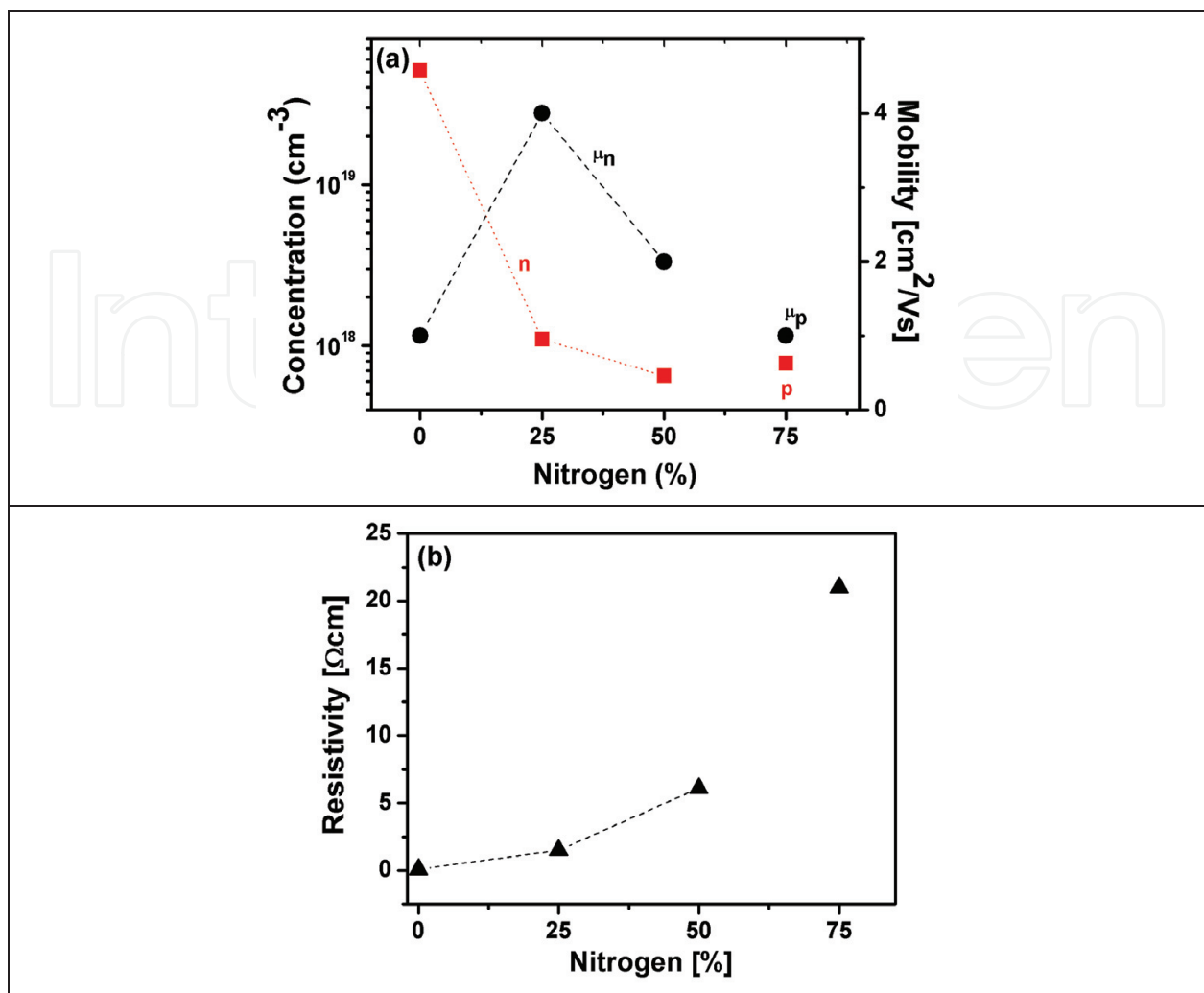


Fig. 11. Effect of the N<sub>2</sub> content on (a) the carrier concentration and mobility and (b) resistivity of ZnO:Al:N films deposited on Corning glass 7059 substrates

The undoped ZnO thin films (0 % N<sub>2</sub> in the sputtering gas) have high resistivity. The minimum resistivity of  $8.9 \times 10^{-2} \Omega\text{cm}$  and the highest carrier concentration of  $5.1 \times 10^{19} \text{ cm}^{-3}$  obtained for ZnO:Al films result from the contribution of the Al<sup>3+</sup> substituents (Al<sup>3+</sup> that substitute for Zn<sup>2+</sup> in the ZnO lattice), in addition to the native donor defects, such as Zn interstitials and O vacancies.

*p*-type conductivity in the ZnO:N thin films and ZnO:N:Al is a result of the nitrogen which substitutes for oxygen in the crystal lattice, creating N<sub>O</sub> acceptors. The incorporation of N<sub>2</sub> was confirmed by means of SIMS depth profiling and Raman - scattering measurements. Besides native donor defects, *p*-type doping in ZnO is limited from the formation of molecules (N<sub>2</sub>)<sub>O</sub> and complexes (N<sub>O</sub> - (N<sub>2</sub>)<sub>O</sub>, N<sub>O</sub> - ZnO) which are the surplus donors to the native ZnO donors.

## 5. Acknowledgements

Presented work was supported by the MSMT Czech Republic project 1M06031 and it has been done in Center of Excellence CENAMOST (Slovak Research and Development Agency Contract No. VVCE-0049-07) with support of project VEGA 1/0220/09, 1/0689/09.

## 6. References

- Assunção, V., Fortunato, E., Marques, A., Águas, H., Ferreira, I., Costa, M. E. V. & Martins, R. (2003). Influence of the deposition pressure on the properties of transparent and conductive ZnO:Ga thin-film produced by r.f. sputtering at room temperature, *Thin Solid Films*, 427, (2003), 401-405
- Carotta, M. C.; Cervi, A., Natale, V., Gherardi, S., Giberti, A., Guidi, V., Puzzovio, D., Vendemiati, B., Martinelli, G., Sacerdoti, M., Calestani, D., Zappettini, A., Zha, M. & Zanotti L. (2009). ZnO gas sensors: A comparison between nanoparticles and nanotetrapods-based thick films, *Sensors and Actuators B*, 137 (2009), page numbers (164-169)
- Delhez, R., De Keijser, Th. H., Mittemeijer, E.J. & Fresenius Z. (1982). *Anal. Chem.*, 312, (1982), 1-16
- Fortunato, E., Assunção, V., Gonçalves, A., Marques, A., Águas, H., Pereira, L., Ferreira, I., Vilarinho, P., Martins, R. (2004). High quality conductive gallium-doped zinc oxide films deposited at room temperature, *Thin Solid Films*, 451 -452, (2004), 443-447
- Fu, E. G., Zhuang, D. M., Zhang, G., Ming, Z., Yang, W. F., Liu, J. J. (2004). Properties of transparent conductive ZnO:Al thin films prepared by magnetron sputtering, *Microelectronics Journal*, 35, (2004), 383-387
- Ganguly, G.; Carlson, D. E., Hegedus, S. S., Ryan, D., Gordon, R. G., Pang, D., Reedy, R. C. (2004). Improved fill factors in amorphous silicon solar cells on zinc oxide by insertion of a germanium layer to block impurity incorporation, *Applied Physics Letters*, Vol. 85, No 3, (July 2004), page numbers (479-481)
- Ge, F. Z., Ye, Z. Z., Zhu, L. P., Lü, J. G., Zhao, B. H., Huang, J. Y., Zhang, Z. H., Wang, L. & Ji, Z. G. (2004). Electrical and optical properties of Al-N co-doped p-type zinc oxide films, *Journal of Crystal Growth*, 268, (2004), 163-168
- Guillén, C., Herrero J. (2006). High conductivity and transparent ZnO:Al films prepared at low temperature by DC and MF magnetron sputtering, *Thin Solid Films*, 515, (2006) 640 - 643
- Hwang, D. K., Kim, H. S., Lim, J. H., Oh, J. Y., Yang, J. H., Park, S. J., Kim, K. K., Look, D. C. & Park, Y. S. (2005). Study of the photoluminescence of phosphorus-doped p-type ZnO thin films grown by radio-frequency magnetron sputtering, *Applied Physics Letters*, 86, (2005), 151917
- Ji, G.; Zhang, Z., Chen, Y., Yan, Sh., Liu, Y. & Mei, L. (2009). Current spin polarization and spin injection efficiency in ZnO-based ferromagnetic semiconductor junctions. *Acta Metallurgica Sinica (English Letters)*, Vol. 22, No. 2, (April 2009), page numbers (153-160)
- Joseph, M., Tabata, H., Saeki, H., Ueda, K. & Kawai, T. (2001). Fabrication of the low-resistive p-type ZnO by codoping method, *Physica B* 302-303, (2001), 140-148
- Kaschner, A., Siegle, H., Hoffmann, A. & Thomsen C. (1999). Influence of doping on the lattice dynamics of gallium nitride, *MRS Internet J. Nitride Semicond. Res.*, 4S1, G3.57, (1999)
- Kraus, I. (1993). *Struktura a vlastnosti krystalů*, ACADEMIA Praha, str. 221
- Lee, E. Ch., Kim, Y. S., Jin, Y. G. & Chang, K. J. (2001). First-principles study of the compensation mechanism in N-doped ZnO, *Physica B*, 912, (2001), 308-310.

- Limpijumnong, S., Li, X., Wei, S.-H. & Zhang, S. B. (2006). Probing deactivations in Nitrogen doped ZnO by vibrational signatures: A first principles study, *Physica B*, 376–377, (2006), 686–689
- Look, D. C., Coşkun, C., Claflin, B. & Farlow, G. C. (2003). Electrical and optical properties of defects and impurities in ZnO, *Physica B*, 340–342, (2003), 32–38.
- Lu, J., Zhang, Y., Ye, Z., Wang, L., Zhao, B. & Huang, J. (2003). p-type ZnO films deposited by DC reactive magnetron sputtering at different ammonia concentrations, *Materials Letters*, 57, (2003), 3311–3314
- Lu, J. G., Fujita, S., Kawaharamura, T. & Nishinaka, H. (2007). Roles of hydrogen and nitrogen in p-type doping of ZnO, *Chemical Physics Letters*, 441, (2007), 68–71
- Lu, J. G., Zhu, L. P., Ye, Z. Z., Zhuge, F., Zeng, Y. J., Zhao, B. H. & Ma, D. W. (2005). Dependence of properties of N-Al codoped p-type ZnO thin films on growth temperature, *Applied Surface Science*, 245, (May 2005), 109–113
- Minami, T., Yamamoto, T. & Miyata, T. (2000). Highly transparent and conductive rare earth-doped ZnO thin films prepared by magnetron sputtering, *Thin Solid Films*, 366, (2000), 63–68
- Moon, T. H., Jeong, M. C., Lee, W. & Myoung J. M. (2005). The fabrication and characterization of ZnO UV detector, *Applied Surface Science* 240, (2005), 280–285
- Nunes, P., Fortunato, E., Tonello, P., Fernandes, F. B., Vilarinho, P. & Martins, R. (2002). Effect of different dopant elements on the properties of ZnO thin films, *Vacuum*, 64, (2002), 281–285
- Ohta, H.; Hosono, H. (2004). Transparent oxide optoelectronics, *Materialstoday*, (June 2004), page numbers (42-51), ISSN:1369 7021 © Elsevier Ltd 2004
- Özgür, Ü., Alivov, Y. I., Liu, C., Teke, A., Reshchikov, M. A., Doğan, S., Avrutin, V., Cho, S.-J. & Morkoç, H. (2005). A comprehensive review of ZnO materials and devices, *Journal of Applied Physics* 98, (2005), 041301
- Park, S. H., Chang, J. H., Ko, H. J., Minegishi, T., Park, J. S., Im, I. H., Ito, M., Oh, D. C., Cho, M. W. & Yao, T. (2008). Lattice deformation of ZnO films with high nitrogen concentration, *Applied Surface Science*, 254, (2008), 7972–7975
- Ryu, Y. R., Zhu, S., Look, D. C., Wrobel, J. M., Jeong, H. M. & White, H. W. (2000). Synthesis of p-type ZnO films, *Journal of Crystal Growth*, 216, (2000), 330–334
- Shtereva, K.; Flickyngerova, S.; Kovac, J.; Tvarozek, V.; Novotny, I.; Skrinjarova, J.; Srnanek, R. & Rehakova, A.; (2008). Preparation of p-/n- type ZnO:Al thin films by RF diode sputtering for solar and optoelectronic applications, *Proceedings of 26<sup>th</sup> International Conference on Microelectronics (MIEL 2008)*, pp. 247 – 250, Nis Serbia, 11-14 May 2008
- Shtereva, K., Tvarozek, V., Novotny, I., Kovac, J., Sutta P. & Vincze A. (2006). p-Type Conduction in Sputtered ZnO Thin Films Doped by Nitrogen, *Proceedings of 25<sup>th</sup> International Conference on Microelectronics (MIEL 2006)*, pp. 357–360, Belgrade, Serbia & Montenegro, 14-17 May 2006
- Song, P. K., Watanabe, M., Kon, M., Mitsui, A. & Shigesato, Y. (2002). Electrical and optical properties of gallium-doped zinc oxide films deposited by dc magnetron sputtering, *Thin Solid Films*, 411, (2002), 82–86
- Sze, S. M. (2002). *Semiconductor devices, Physics and Technology*, John Wiley&Sons, New York, 2002, ISBN 0-471-33372-7
- Sun, J. W., Lu, Y. M., Liu, Y. C., Shen, D. Z., Zhang, Z. Z., Li, B. H., Zhang, J. Y., Yao, B., Zhao, D. X. & Fan, X. W. (2006). The activation energy of the nitrogen acceptor in p-

- type ZnO film grown by plasma-assisted molecular beam epitaxy, *Solid State Communications*, 140, (2006), 345-348
- Šutta, P. & Jackuliak Q. (1998). Macro-stress formation in thin films and its investigation by X-ray diffraction, *Proceedings of 2<sup>nd</sup> International Conference on Advanced Semiconductor Devices and Microsystems (ASDAM'98)*, pp. 227-230, Smolenice Castle, Slovakia, 5-7 October 1998
- Tvarozek, V., Novotny, I., Sutta, P., Flickyngerova, S., Schtereva, K. & Vavrinsky, E. (2007). Influence of sputtering parameters on crystalline structure of ZnO thin films, *Thin Solid Films*, 515, (2007), 8756-8760
- Tvarozek, V., Shtereva, K., Novotny, I., Kovac, J., Sutta, P., Srnanek, R. & Vincze, A. (2008). RF diode reactive sputtering of n-and p-type zinc oxide thin films, *Vacuum*, 82, (2008), 166-169
- Tüzemen, S. & Gür, E. (2007). Principal issues in producing new ultraviolet light emitters based on transparent semiconductor zinc oxide, *Optical Materials*, vol. 30, (2007), 292-310, 2007.
- Van de Walle, Ch. G. (2000). Hydrogen as a Cause of doping in Zinc Oxide, *Physical Review Letters*, 31, vol. 85, No5, (31 July 2000), 1012-1015
- Wang, C., Ji, Z., Xi, J., Du, J. & Ye, Z. (2006). Fabrication and characteristics of the low-resistive p-type ZnO thin films by DC reactive magnetron sputtering, *Materials Letters*, 60, (2006), 912-914
- Wang, Q. J.; Pflügl, Ch., Andress, W. F., Ham, D. & Capasso F., Yamanishi M. (2008). Gigahertz surface acoustic wave generation on ZnO thin films deposited by radio frequency magnetron sputtering on III-V semiconductor substrates. *Journal of Vacuum Science & Technology B*, Vol. 26, No 6, (Nov/Dec 2008), page numbers (1848-1851)
- Xiong, G., Wilkinson, J., Mischuck, B., Tüzemen, S., Ucer, K. B. & Williams, R. T. (2002) Control of p- and n-type conductivity in sputter deposition of undoped ZnO, *Applied Physics Letters*, 80, (February 2002), 7-18
- Yamamoto, T. (2002). Codoping for the fabrication of p-type ZnO, *Thin Solid Films*, 420-421, (2002), 100-106
- Yao, B., Guan, L. X., Xing, G. Z., Zhang, Z. Z., Li, B. H., Wei, Z. P., Wang, X. H., Cong, C. X., Xie, Y. P., Lu, Y. M. & Shen, D. Z. (2007). P-type conductivity and stability of nitrogen-doped zinc oxide prepared by magnetron sputtering, *Journal of Luminescence*, 122-123, (2007), 191-194
- Ye, Z. Z., Ge, F. Z., Lu, J.-G., Zhang, Z. H., Zhu, L. P., Zhao, B. H. & Huang, J. Y. (2004). Preparation of p-type ZnO films by Al+N-codoping method, *Journal of Crystal Growth*, 265, (2004), 127-132
- Ye, Z. Z., Qian, Q., Yuan, G. D., Zhao, B. H. & Ma, D. W. (2005). Effect of oxygen partial pressure ratios on the properties of Al-N co-doped ZnO thin films, *Journal of Crystal Growth*, 274, (2005), 178-182
- Yuan, G., Ye, Z., Zhu, L., Zeng, Y., Huang, J., Qian, Q. & Lu, J. (2004). p-Type conduction in Al-N co-doped ZnO films, *Materials Letters* 58, (2004), 3741-3744
- Zeng, Y. J., Ye, Z. Z., Xu, W. Z., Chen, L. L., Li, D. Y., Zhu, L. P., Zhao, B. H. & Hu, Y. L. (2005). Realization of p-type ZnO films via monodoping of Li acceptor, *Journal of Crystal Growth*, 283, (September 2005), 180-184

- Zhang, S. B., Wei, S. H. & Yan, Y. (2001). The thermodynamics of codoping: how does it work?, *Physica B*, 302-303, (2001), pp.135-139.
- Zhao, J.-L., Li, X.-M., Bian, J.-M., Yu, W.-D. & Zhang, C.-Y. (2005). Growth of nitrogen-doped p-type ZnO films by spray pyrolysis, *Journal of Crystal Growth*, 280, (2005), 495-501
- Zhu, L., Ye, Z., Zhuge, F., Yuan, G. & Lu, J. (2005). Al-N codoping and p-type conductivity in ZnO using different nitrogen sources, *Surface & Coatings Technology*, 198, (2005), 354-356

IntechOpen

IntechOpen

© 2009 The Author(s). Licensee IntechOpen. This chapter is distributed under the terms of the [Creative Commons Attribution-NonCommercial-ShareAlike-3.0 License](https://creativecommons.org/licenses/by-nc-sa/3.0/), which permits use, distribution and reproduction for non-commercial purposes, provided the original is properly cited and derivative works building on this content are distributed under the same license.

IntechOpen

IntechOpen